THE JOURNAL OF PHYSICAL CHEMISTRY C

Article

pubs.acs.org/JPCC

X-ray Photoemission and Density Functional Theory Study of the Interaction of Water Vapor with the Fe_3O_4(001) Surface at Near-Ambient Conditions

T. Kendelewicz,[†] S. Kaya,[‡] J. T. Newberg,[§,#] H. Bluhm,[§] N. Mulakaluri,[⊥,∥] W. Moritz,[⊥] M. Scheffler,[∥] A. Nilsson,[‡] R. Pentcheva,[⊥] and G. E. Brown, Jr.*[,†,‡]

[†]Surface & Aqueous Geochemistry Group, Department of Geological & Environmental Sciences, Stanford University, Stanford, California 94305-2115, United States

[‡]Department of Photon Science and Stanford Synchrotron Radiation Lightsource, SLAC National Accelerator Laboratory, 2575 Sand Hill Road, Menlo Park, California 94025, United States

[§]Chemical Sciences Division, Lawrence Berkeley National Laboratory, Berkeley California 94720, United States

[⊥]Department of Earth and Environmental Sciences, Section Crystallography, University of Munich, Theresienstrasse 41, 80333 Munich, Germany

[∥]Fritz Haber Institute of the Max Planck Society, Faradayweg 4-6, D-14195 Berlin, Germany

ABSTRACT: The interaction of water with the Fe_3O_4(001) surface was investigated in a combined ambient pressure X-ray photoelectron spectroscopy (XPS) and density functional theory (DFT) study. The uptake of molecular water and hydroxyl species on the (001) surface of a natural magnetite sample at near-ambient conditions was quantified using O 1s spectra taken in the p(H_2O) range from 10^{-9} to 2 Torr. At low p(H_2O) ($\leq 10^{-4}$–10^{-5} Torr) and room temperature, we found that water does not adsorb dissociatively on the surface, except on defect sites. In contrast, progressive dissociation into surface hydroxyl species was observed between 10^{-4} and 10^{-2} Torr p(H_2O). The onset of hydroxylation coincides with the increasing presence of molecular water species on the surface, which demonstrates the key role played by cooperative interactions between adsorbed water molecules, leading to dissociation and surface hydroxylation. The measured O 1s chemical shifts of hydroxyl and molecular water species from both isotherm and isobar data are on average ~1.2 eV and ~3.3 eV, respectively, relative to lattice oxygen. The chemical shift of the hydroxyl species on magnetite(001) agrees with previously reported values for hydroxyl species on iron oxyhydroxides such as goethite (α-FeOOH). DFT calculations including an on-site Coulomb repulsion parameter (generalized gradient approximation (GGA) + U approach) predict O 1s surface core-level shifts (SCLS) at the clean $(2^{1/2}\times 2^{1/2})$R45° reconstructed Fe_3O_4(001) surface of up to ~−1 eV depending on the specific bonding configuration of the surface O atoms. Hydroxyl groups formed by the dissociation of isolated water molecules at O vacancies have an SCLS value of ~1.2 eV. With increasing coverage there is a transition toward partial dissociation on the (001) surface. The calculated SCLS for hydroxyl and adsorbed water are 1.2−1.9 and 2.6−3.0 eV, respectively, and compare very well with our experimental results. Final-state effects obtained within the Slater−Janak approach thus have the dominant contribution. In addition, the modest reduction of the work function (~0.5 eV) predicted by DFT calculations for the mixed adsorption of dissociated and intact water molecules agrees well with work function changes measured experimentally. Finally, the similarity between isotherm and isobar data and the DFT calculations for the C-free Fe_3O_4(001) surface indicate that surface hydroxylation is indeed substrate induced and not catalyzed by the presence of adventitious carbonaceous species. Both theory and experiment show the importance of cooperative effects between adjacent water molecules in the dissociation reaction.

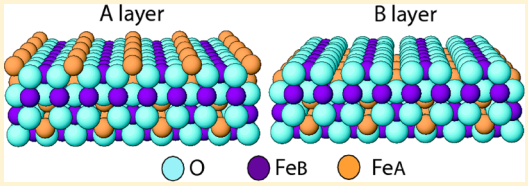

1. INTRODUCTION AND BACKGROUND

The interaction of aqueous solutions with metal oxide surfaces is one of the most important processes occurring in natural and technological systems. These reactions are challenging to study at the atomic level because of the complex structure of the substrates and reactants and other experimental factors, such as surface charging and beam-induced sample damage, which are of importance under reactive conditions. One approach is to identify model systems that can be studied in depth, both experimentally and theoretically, and to gradually build in complexity to simulate more realistic systems. This approach is particularly useful for iron oxides, hydroxides, and oxyhydroxides, which have diverse structures and electronic properties. Here we use ambient-pressure X-ray photoelectron spectroscopy (APXPS) to study interactions of pure molecular water vapor with a vacuum-prepared (001) surface of magnetite. To gain understanding of the observed trends, the

Received: August 6, 2012
Revised: December 27, 2012
Published: January 16, 2013

   dx.doi.org/10.1021/jp3078024 | *J. Phys. Chem. C* 2013, 117, 2719–2733

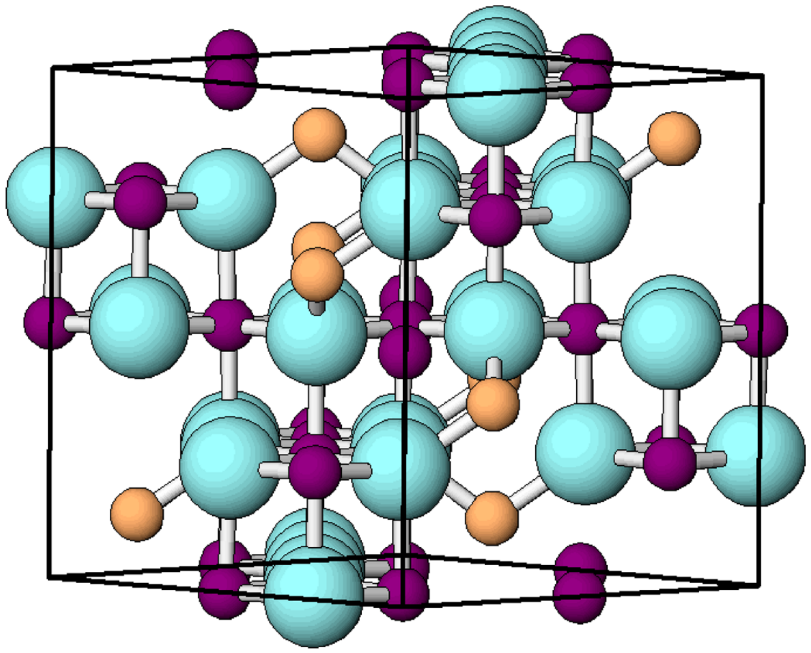

Figure 1. Side view of the magnetite(001) surface along the [110] direction. Tetrahedral and octahedral iron atoms and oxygen atoms are in orange (medium gray), purple (dark gray), and cyan (light gray), respectively.

O 1s core-level shifts and work function changes were calculated using DFT at the GGA+*U* level.

Magnetite is a common accessory mineral in igneous and metamorphic rocks and also occurs in sediments and soils as a weathering product; thus, this phase is important in geoscience and soil science and is the most common naturally occurring magnetic phase. In nature, magnetite plays a role in a variety of biotic redox reactions.[1] It is also an important sorbent and reducing agent of toxic metals and metalloids and other contaminants in aqueous environments.[1] For example, it has recently been shown that magnetite reduces Hg(II) to Hg(0).[2] Interfacial phenomena related to aqueous reactions with mineral surfaces such as magnetite are thus of interest in water treatment as well as in corrosion prevention. The prediction of half-metallic behavior in bulk magnetite and recent success in the epitaxial growth of high quality ordered Fe_3O_4 films made magnetite a prospective material in the field of spintronics, which exploits the spin of charge carriers to produce new types of electronic devices.[3] Magnetite is also a model for a correlated magnetic material, and significant efforts have been directed at understanding the nature of the low temperature Verwey phase transition (or, in general, metal−insulator transitions).[4] Above the Verwey temperature of ∼125 K, Fe_3O_4 is a conductor with an inverse spinel structure in which O^{2-} ions form a slightly distorted cubic close-packed or fcc structure and the Fe ions occupy two types of interstitial sites (see Figure 1). The lattice constant is 8.396 Å,[5] and the unit cell contains 32 oxygen and 24 Fe atoms. One third of the Fe ions in the form of Fe^{3+} occupy 8 (of 64) tetrahedrally coordinated "A sites", whereas the remaining two-thirds of the Fe ions occupy 16 (of 32) octahedrally coordinated "B sites" with equal numbers of Fe^{2+} and Fe^{3+} ions. Electron hopping along the octahedral iron chains (i.e., along crystallographically equivalent [110] directions) is responsible for the bulk conductivity of magnetite over a broad range of temperatures.[4]

Understanding of the most common magnetite surfaces (the (001) and (111) orientations) is also of importance because of their roles in adsorption reactions of toxic heavy metals in Earth surface environments. The reconstructed (001) magnetite surface has been the subject of spectroscopic, diffraction, and scanning tunneling microscopy (STM) studies over the past two decades (e.g., see refs 6−26), as well as recent DFT calculations.[27−30] As shown in Figure 2, the (001) surface can

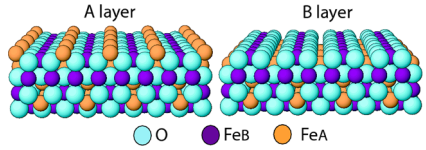

Figure 2. Side view of the bulk terminations of Fe_3O_4(001) with an A-layer of tetrahedral iron or a B-layer containing octahedral iron and oxygen. For color-coding, see Figure 1.

expose two distinct terminations with either tetrahedral (orange) or octahedral (purple) Fe atoms and oxygen (cyan). In the literature these terminations are commonly labeled as A- and B-layers, respectively. Whereas the A termination contains solely tetrahedral ferric ions, the B termination, in addition to mixed valence (ferric and ferrous) octahedral ions, also contains oxygen atoms (purple). Layers A and B, with antiferromagnetically coupled magnetic moments of iron ions and spaced by 1.05 Å, repeat cyclically along the [100] direction. In the bulk the distance between A−A or B−B planes, is 2.1 Å or 1/4 of a unit cell. Each layer within a (bulk) unit cell has a formal charge of +6 (two tetrahedral irons) or −6 (eight oxygens and four octahedral irons with an average valence of +2.5), making both surface terminations polar.[31] Polar surfaces are considered to be energetically unstable and prone to reconstruction, which typically involves vacancy formation and/or adsorption of foreign species, including hydroxyls.[32] The stability of metal oxide surfaces is usually assessed using the equivalent criteria of autocompensation[33] or polarity.[31,32] These two criteria have also been applied in prior studies of magnetite to unravel the nature of the $(2^{1/2}\times2^{1/2})R45°$ reconstruction for the (001)

dx.doi.org/10.1021/jp3078024 | J. Phys. Chem. C 2013, 117, 2719−2733

surface. This reconstruction occurs over a broad range of preparation conditions for (001) terminations of Fe_3O_4 single crystals (both natural and synthetic) and vacuum-grown (001) epitaxial layers. However, in the case of transition metal oxides, further electronic-driven mechanisms, such as charge redistribution and localization, can occur instead of the more common atomic reconstruction described above.[34] Indeed, recent DFT calculations have shown that the lowest surface energy is obtained by a distortion of the ideal B-terminated surface.[27,29,30] At low oxygen pressures, a termination with oxygen vacancies is stabilized.[30]

Understanding the interaction of water with the magnetite(001) surface is of key importance for most technological applications in spintronics, environmental science, and catalysis. It is therefore surprising that only a few studies have been carried out on the interaction of water with the Fe_3O_4(001) surface to date. Our previous room temperature ultrahigh vacuum (UHV) XPS study of oxygen 1s core-level shifts found two water adsorption regimes:[35] At low water vapor pressures, the data were interpreted as indicating dissociative chemisorption activated by surface defects. Above water vapor pressures of 10^{-3} to 10^{-4} mbar, extensive hydroxylation of surface oxygens was observed. This onset pressure for extensive H_2O adsorption and dissociation is similar to values reported for the Fe_3O_4(111)[35] and α-Fe_2O_3 (0001) surfaces.[36] A broad feature at 1.6 eV lower than the main O 1s XPS oxide peak was attributed to hydroxyl groups at nonequivalent sites. Furthermore, no sign of formation of a surface oxyhydroxide phase was found in near edge extended X-ray adsorption fine structure (NEXAFS) spectra at the Fe *L*-edge.[35] Temperature-programmed desorption (TPD) experiments[37] on epitaxially grown Fe_3O_4(001) thin films on MgO(001) substrates detected three desorption peaks at 320 K, 280 K, and 225 K. These were attributed to different chemisorbed states, but the exact adsorbate configurations and their relative stabilities could not be directly determined from experiment alone. In contrast, a recent STM study[38] suggests that dissociative adsorption of water on the Fe_3O_4 (0001) surface at room temperature results only in hydrogenation of surface oxygens, resulting in the reduction of the surface under UHV conditions, with the remaining OH groups leaving the surface, possibly in the form of H_2 and O_2. These results will be addressed in Discussion.

On the theoretical side, water adsorption on Fe_3O_4(001) has been studied by molecular dynamics (MD)[39,40] using empirical potentials. These studies indicate that water interacts with this surface by dissociative chemisorption. However, water adsorption was modeled using a termination with a 0.5 ML (monolayers) of tetrahedral iron (0.5 A-layer), which according to DFT calculations[27,29] is energetically unfavorable. Instead a distorted B-layer termination is stable over a broad range of oxygen pressures, as also confirmed by X-ray diffraction and low energy electron diffraction (LEED) experiments.[27] Recently, a surface phase diagram of the interaction of water with the Fe_3O_4(001) surface as a function of the oxygen and water chemical potentials was derived[30,41] in the framework of ab initio atomistic thermodynamics.[42,43] The results show that at low oxygen and water pressures, isolated water molecules dissociate at surface defect sites (oxygen vacancies). With increasing concentration of adsorbed water molecules, these defects are no longer required, due to water−water interactions, and a crossover to partial dissociation takes place. This gives rise to a mixed adsorption mode that is stabilized by the formation of hydrogen bonds between OH groups and H_2O molecules adsorbed at adjacent Fe_B sites.

To gain further insight into the mechanism and coverage dependence of water adsorption on Fe_3O_4(001), we have calculated here the O 1s surface core-level shifts (SCLS) using DFT, taking into account both initial- and final-state effects, and we compare these SCLS with our XPS measurements. The paper is structured as follows: After providing a brief description of the experimental and theoretical approaches (section 1), we present the XPS (section 2a) and DFT results (section 2b) followed by experimental and theoretical results in section 3a and section 3b, respectively. Section 4 provides a discussion of the main findings including a comparison with those for other iron oxide surfaces. Finally, the results are summarized in section 5.

2. EXPERIMENT AND ANALYSIS

2a. XPS. Experiments were performed in the APXPS chamber at undulator beamline 11.0.2 of the Advanced Light Source (ALS) at Lawrence Berkeley National Laboratory. Details of the beamline and experimental end station are presented elsewhere.[44,45] In short, the experimental system consists of two interconnected UHV chambers with base pressures of $\sim 2 \times 10^{-10}$ Torr and a fast entry sample load lock stage. Sputter gun and LEED optics in the preparation chamber are used for surface cleaning and control of the surface structure. The analysis chamber is equipped with a Specs Phoibos150 hemispherical analyzer with differentially pumped electron lens and a set of ionization, convectron, and Baratron pressure gauges used to control pressure during experiments. All necessary gases are introduced via variable leak valves from a clean gas distribution system. Prior to water dosing, Milli-Q water was degassed by multiple freeze−pump−thaw cycles. Water pressures were monitored with ionization and convectron gauges for pressures up to 10^{-4} and 10^{-2} Torr, respectively. At the highest pressure, the Baratron gauge provided the most reliable control.

We used a natural magnetite crystal from Zillertal, Austria, with an (001) termination. The crystal was cut with a diamond wire saw and was oriented with an X-ray diffractometer to within 0.5° of the (001) plane and polished to yield a sample of $\sim 10 \times 12$ mm in size. Sample composition was determined by X-ray fluorescence spectroscopy, showing 1% Mn contamination. The sample was mounted on a molybdenum plate located above a button heater. The surfaces were prepared by several cycles of Ar^+ (1 kV) sputtering and annealing in 5×10^{-7} Torr of O_2 at 773−923 K for ∼10 min. The temperature was monitored using a chromel−alumel thermocouple welded to the holder at the edge of the sample. This procedure resulted in the healing of any Ar^+ ion sputtering-induced defects and restoration of long-range ordering. After the annealing step, the samples were cooled in the same oxygen ambient, preventing temperature-induced reduction of the Fe_3O_4(001) surfaces, as checked by Fe $2p_{3/2}$ XPS spectra, which are consistent with magnetite and not wüstite (FeO) (spectra not shown). After cleaning, the sample displayed a sharp $(2^{1/2}\times 2^{1/2})$R45° LEED pattern, which was uniform over the whole sample. This homogeneity is important because in order to avoid beam damage in spectroscopic experiments we often changed sample position. Structural or compositional nonuniformity of the surface could lead to spurious results. The contamination, in particular the presence of adventitious carbon species, was systematically controlled during the experiments. Several core-

dx.doi.org/10.1021/jp3078024 | J. Phys. Chem. C 2013, 117, 2719−2733

level spectra, including O 1s, C 1s, Fe 2p, and valence band spectra were acquired during the course of these experiments. Photon energies for all core levels were chosen to yield photoelectrons with kinetic energies of ∼150 eV, and thus all measurements had the same surface sensitivity. In this paper we concentrate on the O 1s spectra, which provide key information on hydroxylation and water adsorption on the surface. The O 1s spectra were decomposed into components of a combined Gaussian−Lorentzian shape using CasaXPS software.

At the end of each set of O 1s measurements, we repeated the measurements to evaluate potential beam damage and slower kinetic effects. Synchrotron beam-induced effects on the spectra were observed in our prior ex situ XPS study of the reaction of water with the magnetite(111) surface[35] and in in situ XPS studies of the interaction of water vapor with thin MgO(001) layers grown on Ag(001).[46] The latter experiments were carefully repeated once the problem was recognized. Therefore, as a precaution against beam-induced effects, each O 1s spectrum presented in this work was taken at a new sample position. It is worth noting that an a posteriori inspection of the data from the magnetite(001) experiment showed no noticeable beam damage, i.e., O 1s spectra at the beginning and at the end of each spectral series remained unchanged after ∼7 min beam exposure (this observation also eliminates the possibility of slower kinetic changes on the water-dosed surface). However, by changing the beam position (∼0.5 mm, i.e., more than the beam size) for every new pressure point, we likely avoided the cumulative effects of prolonged beam exposure. The validity of the above-mentioned rastering procedure relies on the assumption of perfect homogeneity of the surface. Indeed, after repeated sample preparation and for hundreds of sample positions, we found only a few spots, typically close to the sample edges, that showed discontinuous spectral behavior. These uncertain data were checked by taking a spectrum on an additional spot. As already mentioned, a perfect LEED superstructure was routinely observed over the whole surface of this natural magnetite crystal.

We used a multilayer model that assumes exponential attenuation of the photoemission with depth (Beer−Lambert Law)[46,47] to get estimates of the thickness of hydroxyl and water vapor layers from the intensities of O 1s photoemission peaks. In the case where both water and hydroxyl ions are present on the surface, the O 1s emission intensity from the topmost water layer is given by the following formula:[46,48]

$$I_{H_2O} \sim \rho_{H_2O}\sigma_{H_2O}\lambda_{H_2O} \sin\Theta[1 - \exp(-t_{H_2O}/\lambda_{H_2O} \sin\Theta)]$$

where ρ_{H_2O}, σ_{H_2O}, λ_{H_2O}, and t_{H_2O} are the atomic density, photoemission cross section, escape depth, and layer thickness, respectively. The emission angle is measured from the surface plane. The intensity of photoemission from the OH layer just underneath this topmost water layer is given by:

$$I_{OH} \sim \rho_{OH}\sigma_{OH}\lambda_{OH} \sin\Theta[1 - \exp(-t_{OH}/\lambda_{OH} \sin\Theta)] \exp(-t_{H_2O}/\lambda_{H_2O} \sin\Theta)$$

where the last exponent represents attenuation of intensity from hydroxyl groups by the topmost layer of water. A similar but simplified formula applies to the O 1s emission from the semi-infinite ($t_b \to \infty$) bulk oxide intensity (I_b), which in turn is attenuated by both hydroxyl and water layers. The thicknesses of OH (t_{OH}) and H_2O (t_{H_2O}) can be obtained by dividing I_{OH} and I_{H_2O} by I_b and solving for these two unknowns. The model assumes that the layers are uniform in thickness and neglects vertical relaxation or changes thereof upon deposition of the water overlayer. A more complete discussion of the layer model can be found in the literature (e.g., refs 46, 47, and 49). The parameters used in the model are discussed in a recent XPS study of the water/hematite interface by Yamamoto et al.[47] The layer thicknesses, which are determined in length units of Å, are converted to ML by dividing the calculated values by 3.02 Å[50] and 3.1 Å[50] for OH and H_2O, respectively. These values correspond to the lattice constant of bulk goethite[51] and a one monolayer slice of water given by the cube-root of its bulk density at room temperature, respectively.

2b. DFT Calculations. Density functional theory calculations were performed using the Wien2k code.[52] As an all-electron code it treats explicitly the core electrons and thus allows direct access to Kohn−Sham energy eigenvalues of a particular core state for the evaluation of SCLS as discussed below. For magnetite as a strongly correlated system, we have considered electronic correlations beyond the generalized gradient approximation[53] by an additional on-site Coulomb repulsion term[54] with U = 5 eV and J = 1 eV applied on the Fe 3d states. Similar values were previously used to describe the low temperature phase of bulk Fe_3O_4.[55,56] Using these values, GGA+U predicts the opening of an insulating band gap[29,30] at the Fe_3O_4(001) surface, consistent with scanning tunneling spectroscopy measurements.[57] The Fe_3O_4(001) surface is modeled by a slab containing seven B-layers and six A-layers as described previously.[30,41] The muffin-tin (MT) radii are R_{MT}^{Fe} = 1.90, R_{MT}^{O} = 1.10, and R_{MT}^{H} = 0.60 Bohr. Mixed augmented plane wave (APW+lo) and linear augmented plane wave (LAPW) basis sets were employed. Inside the MT spheres the wave functions are expanded in spherical harmonics up to l_{wf}^{max} = 10. Nonspherical contributions to the electron density as well as to the potential are considered up to l_{pot}^{max} = 6. The energy cutoff for the plane wave representation and potential are E_{wf}^{max} = 25 Ry and E_{pot}^{max} = 196 Ry, respectively. For the integration in the Brillouin zone, 16 $k_{||}$-points were used. For further computational details, see refs 30 and 41.

SCLS is defined as the difference in energy required to remove a core electron from a bulk atom versus a surface atom[58] and consists of two contributions: an *initial-state effect* which reflects the difference in core-level of the ion in the surface versus bulk before excitation of the core hole, and a *final-state effect,* which is due to different screening effects of the core-ionized system in the bulk vs the surface.[58] Although experiments provide the total shift, the DFT calculations allow us to distinguish between the two contributions, which is useful in the interpretation of experimental results. The initial-state shifts are calculated as the change in the core orbital energies (Kohn−Sham orbital energies) between ions in the surface layer and in the bulk. All the energy eigenvalues are calculated with respect to the Fermi level of the respective system. Final-state screening is considered using the Slater−Janak transition state approach,[59−62] where a core hole is created at a bulk and a surface atom by transferring half an electron from the core to the valence level. This is an excellent approximation for the total energy difference of the N and $N - 1$ electron systems.[63] The calculations for the bulk atom were performed separately in a cubic bulk unit cell of magnetite with 56 atoms where the distance between the ionized cores is 8.41 Å to minimize the interaction.

dx.doi.org/10.1021/jp3078024 | J. Phys. Chem. C 2013, 117, 2719−2733

3. RESULTS

3a. Experimental Results. Figures 3a and 3b present O 1s photoemission spectra from a $(2^{1/2}\times2^{1/2})$R45° (001) magnetite

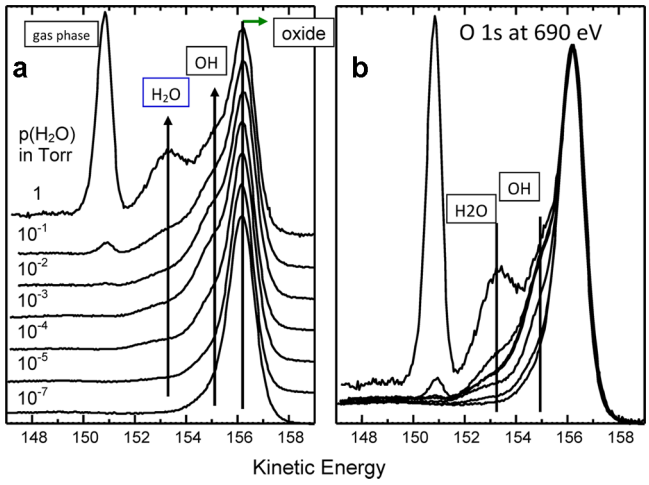

Figure 3. (a) Height-normalized O 1s spectra from a $(2^{1/2}\times2^{1/2})$R45° surface of magnetite(001) held at 273 K and exposed to increasing water vapor pressures (bottom to top) given in Torr. (b) Same data redrawn to enhance changes in the OH and adsorbed H_2O components shifted by ∼−1.4 and ∼−3.3 eV relative to the substrate's O 1s component at the highest kinetic (lowest binding) energy. The peak on the far left side at the highest water vapor pressures results from the gas -phase water in the chamber, which is excited by the synchrotron radiation between the sample and the analyzer's lens nozzle.

surface exposed to water vapor. The spectra in Figure 3 were arbitrarily normalized to constant height of the bulk substrate O 1s feature. The experiment from which these spectra were derived was performed in an isotherm mode, with the surface held at 273 K. The $p(H_2O)$ was increased in steps of roughly 1 order of magnitude starting from 5×10^{-9} Torr up to 1 Torr. Not included are data obtained below 10^{-7} Torr $p(H_2O)$, which closely resemble data from the clean surface. At each pressure, a set of spectra including O 1s, Fe 2p, valence band (VB), and C 1s were taken.

At $p(H_2O)$ values of up to 10^{-7} Torr and 273 K, the O 1s spectra are adequately represented by a single peak representing lattice oxygens (Figure 3). A slight asymmetry of this peak, seen as a low kinetic energy tail, has been observed in previous studies and is discussed in the literature (e.g., see refs 11, 64, and 65). Some authors associate this tail with residual hydroxylation of the UHV-prepared "clean" surfaces, while others assign it to final-state losses (shakeup).[11] Although the O 1s tail was observed by most authors, an interesting precedent was set by the work of Fujii et al.,[66] who reported symmetric O 1s XPS spectra for several epitaxially grown iron oxides, including magnetite. Although the origin of the tail is not conclusively established, trace residual hydroxylation cannot be excluded under most preparation conditions. Indeed, DFT calculations indicate that surface oxygen vacancies bind hydroxyl species very strongly.[30,41]

At ∼10^{-5} Torr, $p(H_2O)$, a new feature, shifted by ∼−1.2 eV, starts to grow on the low kinetic side of the bulk O 1s spectrum (Figure 3). We attribute this additional component to hydroxyl species in excess of possible vacancy-bound hydroxyls. The position of the hydroxyl peak is marked with a solid line in Figure 3. At ∼10^{-2} Torr, as the intensity of the OH component reaches a plateau, a third component grows rapidly at ∼−3.3 eV below the O 1s substrate peak. We attribute this peak to surface-bound molecular water, which eventually condenses, forming thicker layers on the surface at higher relative humidity (RH) values.[67] Molecular water seems to already be present on the partially hydroxylated magnetite(001) surface at low pressures, but adsorption of water does not precede hydroxylation. This observation agrees with prior low-temperature XPS and APXPS studies, which stresses the role of OH groups in anchoring surface water via hydrogen bonding.[68] An additional photoemission peak in Figure 3 at high $p(H_2O)$, which grows in intensity at a much lower kinetic energy, is attributed to unbound gas-phase water present in the chamber, which is excited between the probed surface and the analyzer's lens nozzle by the incident beam. Electron scattering in gas-phase water significantly reduces the intensity of the surface and interface peaks and thus increases noise in the normalized spectra. In fact, although we can increase $p(H_2O)$ above 1 Torr, it is difficult to acquire good quality and contaminant-free data within a reasonable time. Adventitious carbon contains oxygenated components, which complicate quantitative O 1s data analysis. In the present experiment the highest water vapor pressure was 2.1 Torr which, at 273 K, corresponds to ∼45% RH.

Figure 4 shows O 1s data acquired for the same pressures as in Figure 3 during a stepwise evacuation of water from the

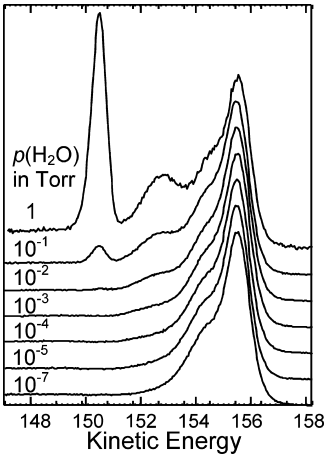

Figure 4. Height-normalized O 1s spectra from a $(2^{1/2}\times2^{1/2})$R45° surface of magnetite(001) held at 273 K and exposed to the maximum water vapor pressure of 1 Torr (top spectrum). The consecutive spectra (top to bottom) were obtained during controlled stepwise pump down. The pressures correspond to those of Figure 3 but were obtained in a reverse order (top to bottom).

chamber after exposure of the surface to 1 Torr $p(H_2O)$. The results show fast reversible removal of adsorbed water during evacuation. However, the surface appears to remain hydroxylated as evidenced by the intensity of the OH component, with a 1.1 eV chemical shift. The last spectrum in this sequence is the only data point accessible in the traditional UHV set up, where dosing is conducted in a separate sample preparation chamber.[35]

The data presented in Figures 3 and 4 have been confirmed by measuring two additional pressure-up and pressure-down isotherms conducted at room temperature (data not shown). The 351 K isotherm, which covers a narrower range of partial

dx.doi.org/10.1021/jp3078024 | J. Phys. Chem. C 2013, 117, 2719−2733

water pressures up to only RH = 0.2% (at 0.7 Torr water pressure), is similar but shows much less molecular water on the surface. This small RH is, however, sufficient to fully hydroxylate the magnetite(001) surface. In all cases the data indicate a homogeneous distribution of reaction products over the whole sample, as determined by measuring spectra at a number of different sample locations.

In addition to the isotherms, we measured several isobars for $p(H_2O)$ between 0.005 and 1 Torr and for temperatures decreasing from ~+573 K to ~266 K, which correspond to RHs of $\sim 10^{-5}$ % to 37%. Isobaric measurements were conducted by leaking water vapor up to the final pressure on a hot clean sample (just after preparation) and then reducing the temperature within several hours in a stepwise fashion using a chiller. No spectra other than O 1s and C 1s were taken. In contrast with the isotherm data, where the presence of small amounts of C contamination could not be avoided at the highest $p(H_2O)$ values, the isobar data are almost free of C contamination. Figure 5 shows the O 1s spectra from two sets

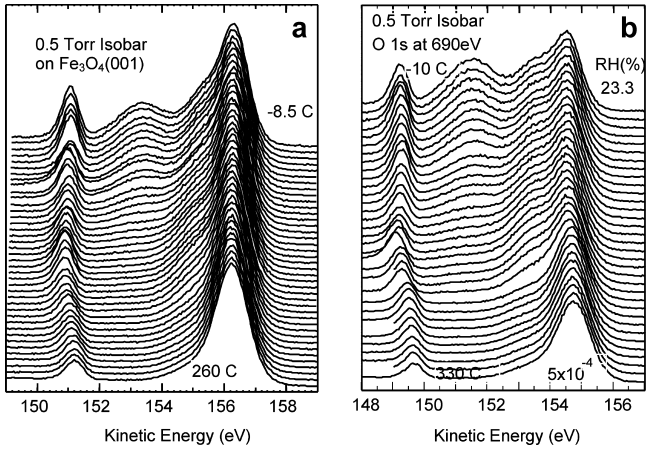

Figure 5. O 1s core-level spectra from two 0.5 Torr water pressure isobars taken on the $(2^{1/2}\times 2^{1/2})$R45° surface of magnetite(001). The data were acquired in the temperature range from (a) 260 °C to −8.5 °C and from (b) 330 °C to −10 °C. The latter temperature range corresponds to relative humidities between 5×10^{-4}% and 23% and covers all important stages of water interaction on the magnetite(001) surface.

of 0.5 Torr isobars, which cover a RH range from 5×10^{-4} to 23%, i.e., the range where hydroxylation and molecular water uptake occur as the temperature is reduced. The advantage of the isobar data is that all of the spectra could be taken on samples free of surface contamination. Because the isobar and isotherm data show qualitatively similar trends, we conclude that surface hydroxylation is not catalyzed by the presence of spectator carbonaceous species.

More detailed information on the reaction of water with magnetite(001) comes from spectral decomposition of the O 1s data. Figure 6a shows examples of curve fits for selected O 1s spectra from the 0.5 Torr isobar shown in Figure 5. All the data from isobars and isotherms were decomposed in the same fashion using CasaXPS software to derive respective peak intensities and chemical shifts of the contributing features. During fitting we tried to impose as few constraints as possible. Separation of the bulk and hydroxyl components did not pose a serious problem during fitting, despite a small chemical shift and large widths of these features.

Some care had to be taken when including the water peak at the very onset of water accumulation. The elimination of this peak can be easily compensated for by a small adjustment of the background and/or an increase of width for the hydroxyl-related feature. In some cases the water component had to be constrained in width and/or position by extrapolating its widths and energies from the regime of higher water coverage, where the need to use the water feature in the fits is firmly established in the data. In the next step of data reduction, the layer model, described in Experiment and Analysis, was implemented to derive estimates of the coverages of hydroxyl and water species on the surface. Figure 6b presents results of the analysis for the 0.5 Torr isobar data of Figure 5a and 5b. For comparison, the data are plotted on both logarithmic and linear scales in Figure 6b. Particularly instructive is the logarithmic plot, which shows a clear onset of hydroxylation at a RH of 0.01%. On this scale, OH uptake quickly saturates at a coverage of ~1 ML. In addition, the onset of water uptake seems to coincide with the onset of hydroxylation, but the increase of water coverage is more gradual, and one ML coverage is reached at a relative humidity of a few percent. To determine how general our observation is, Figure 7 compares results from four isobars ($p(H_2O)$ between 0.005 and 1 Torr) taken in the same experimental run on similarly prepared samples. In all cases we observed an onset of hydroxylation near an RH of 0.01%, which was quickly followed by or coincided with the uptake of molecular water. With the exception of the 0.005 Torr isobar with a maximum RH of only 0.15%, all isobars indicate maximum hydroxyl coverage of ~1 ML. We also observed a more or less pronounced knee in the water uptake at a RH of ~0.1%. This "knee" perhaps distinguishes between water bound to hydroxyls versus molecular water that is more abundant on the surface at higher relative humidities.

The O 1s isobars collected at higher $p(H_2O)$ (where the water gas-phase peak is present) allow one to estimate relative changes of the work function (WF) of the magnetite surface at different stages of its reaction with water. This change is derived from the energy difference between the substrate O 1s and gas-phase O 1s peaks. Although the energy of the lattice O 1s is pegged to the substrate's Fermi level (valence band maximum), the energy of the gas-phase O 1s is fixed relative to the vacuum level.[69] Figure 8 shows changes of the WF determined in this manner for two 0.5 Torr isobars from Figure 5. The energy difference at the starting RH serves as the zero energy reference (the absolute value of the work function cannot be determined in our experimental setup). The two curves show reproducibly that a reduction of the work function by 0.5 eV occurs at a RH of 0.01% and thus coincides with the onset of hydroxylation. This reduction indicates that adsorbates are bound with O pointing down toward the surface. For higher RHs, a slight increase of the WF indicates depolarization of the surface dipole as more and more water molecules reside on the magnetite(001) surface.

Some other characteristics of the interface can be extracted from the spectral data. In Figure 9 we show changes of width (fwhm) of the bulk O 1s magnetite component as a function of RH. For all the interfaces studied, we observed a reduction of the width of this peak as a function of RH or $p(H_2O)$. We suggest that this effect is due to unrelaxation of the substrate in the presence of hydroxyl and water on the surface. Significant relaxations of the surface O atoms on the reconstructed clean surface from the bulk positions were found in a combined DFT and LEED study,[70] resulting in noticeable surface chemical shift

dx.doi.org/10.1021/jp3078024 | J. Phys. Chem. C 2013, 117, 2719−2733

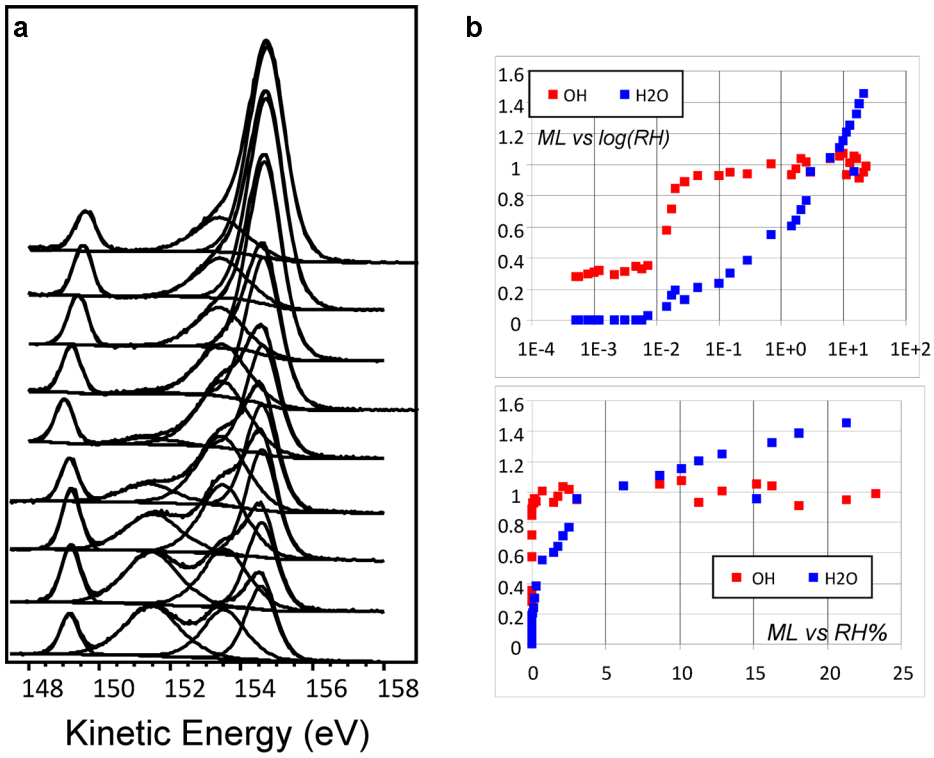

Figure 6. (a) Example of data analysis for a 0.5 Torr isobar using raw data presented in the left panel of Figure 5, which ranges from −8.5 °C (bottom spectrum) to 260 °C (top spectrum). The data are decomposed into spectral components representing gas-phase H_2O, adsorbed H_2O, OH, and bulk lattice oxygen (left panel). In the next step, a layer model (described in Experiment and Analysis) is applied to estimate coverages of these species. (b) The results are plotted as a function of relative humidity on logarithmic (top panel on the right) or linear scale (bottom panel on the right). From the linear scale plot, it is clear that reactions take place at very small relative humidities. The logarithmic scale plot clearly yields an onset of hydroxylation at a RH ∼ 0.02%.

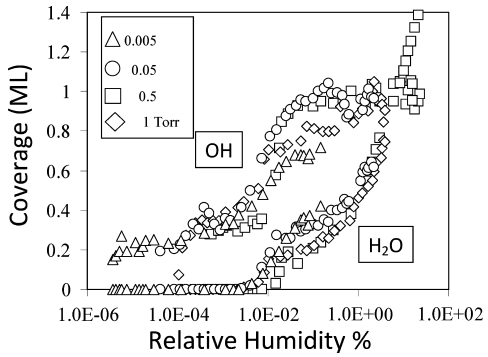

Figure 7. Changes of the coverage of hydroxyls and molecular water species in ML estimated using a layer model from representative isobars. The data are presented as a function of relative humidity in percent.

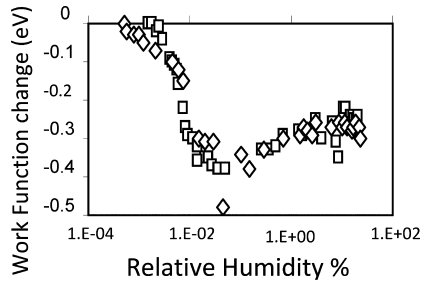

Figure 8. Change of the work function for the magnetite(001) surface exposed to water vapor determined from the energy difference between the bulk O 1s magnetite oxide component and the gas-phase water O 1s measured in the same spectrum. The 0.5 Torr isobar data used for this derivation are shown in Figure 5. The symbols are the same as those defined in Figure 7.

(see Theoretical Results). Recent DFT and LEED results show that upon water adsorption the ions relax back close to their bulk positions and there are indications of a lifting of the $(2^{1/2}\times2^{1/2})$R45° reconstruction.[30] Similarly, small changes in relaxation due to the presence of water (both dissociated and undissociated) were observed in a crystal truncation rod X-ray diffraction study of the hydrated (111) surface of magnetite,[71] which also showed two distinct types of surface domains, one with octahedral iron atoms at the surface (comprising 75% of the surface) and one with both octahedral and tetrahedral iron (comprising 25% of the surface). The chemical shift is difficult to establish directly because the O 1s peak in all oxides, including conducting magnetite, is very broad. However, adsorption of capping species can cause the peak to narrow when the unresolved surface component is eliminated. The fwhm values of hydroxyl and molecular water species were also determined and vary on average between 1.6 and 1.9 eV without an obvious systematic trend. In Figure 10 we present chemical shifts of hydroxyl and water species relative to the bulk oxide peak as a function of RH. In both cases we observe a decrease of the chemical shift values. In the isobars, the OH-related shift decreases from 1.4 to 1.0 eV for the highest water doses, whereas the H_2O shift decreases from 3.5 to 3 eV.

3b. Theoretical Results. To understand the measured XPS shifts, we calculated the O 1s SCLS of oxygen atoms in the top surface layer of the clean Fe_3O_4(001) surface and of adsorbed

dx.doi.org/10.1021/jp3078024 | J. Phys. Chem. C 2013, 117, 2719−2733

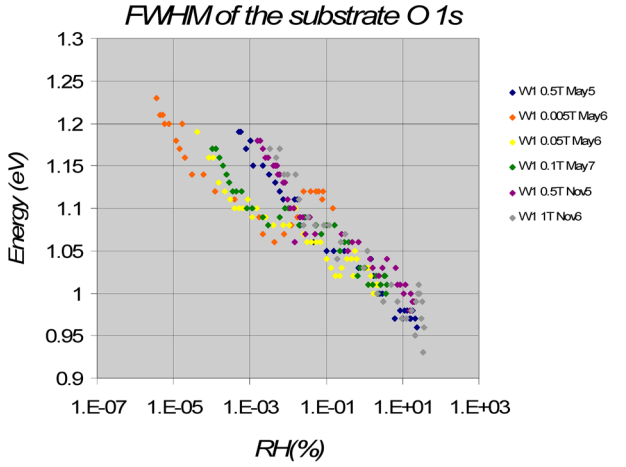

Figure 9. Change of width (fwhm) of the bulk oxide component of the O 1s spectrum as a function of relative humidity. For clarity, data are from isobars only; results from isotherms are consistent, so the effect is not just the result of reduced temperature.

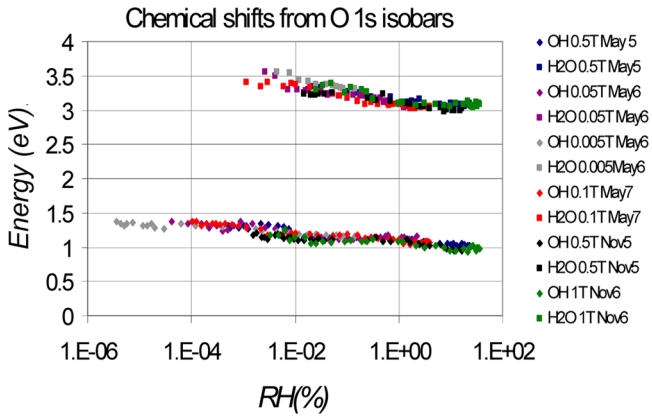

Figure 10. Changes of O 1s chemical shifts of hydroxyl and molecular water species relative to the bulk oxide peak as a function of relative humidity.

water molecules and hydroxyl groups. In particular, we considered four stable terminations that dominate the surface phase diagram[30] obtained in the framework of ab initio atomistic thermodynamics:[43] for the clean surface, the modified B-layer termination, which is most favored over a broad range of oxygen pressures,[27,29,30] and a B-layer with oxygen vacancies (V_O) that is stabilized under oxygen-poor conditions. The relevant configurations upon water adsorption include an isolated water molecule dissociated in an oxygen vacancy, thus forming two surface OH groups ($1D_V$), and a B-layer with two (2M) and four H_2O molecules (4M) at higher water coverages. Previous calculations have shown that with increasing coverage, the mixed adsorption mode (M) is favored where half of the molecules remain intact and the other half dissociate. This configuration is stabilized via formation of hydrogen bonds and is 0.39 eV more favorable than complete dissociation of the water molecules. A top view of the stable configurations is shown in Figure 11, and the corresponding O 1s SCLS are listed in Tables 1 and 2. Further information on the energetic stability and structural and electronic properties can be found in Mulakaluri et al.[41]

The sign convention used here is such that a negative/positive SCLS means a shift toward lower/higher binding

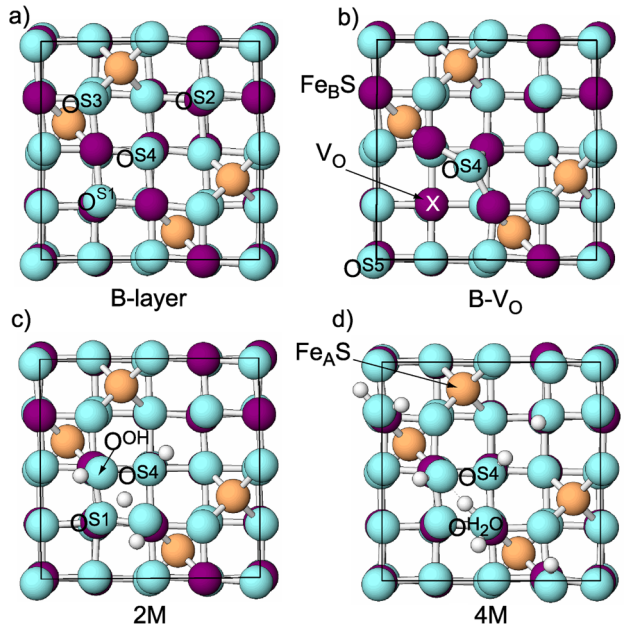

Figure 11. Top views of the stable surface terminations for which surface core-level shifts were calculated: (a) modified B-layer, (b) B-layer with an oxygen vacancy (B−V_O), B-layer with (c) 2 and (d) four H_2O molecules in mixed adsorption (4M). O^{S1-S5} label different surface oxygen ions, while O^{OH} and O^{H_2O} denote oxygen of a hydroxyl group and water molecule on top of FeB, respectively. The positions of FeB, FeA, O, and H are indicated by purple, orange, cyan, and white circles.

Table 1. O 1s SCLS on the Clean $Fe_3O_4(001)$ (in eV) for Two Different Clean Surface Terminations: The Modified B-Layer and a B-Layer with Oxygen Vacancies[a]

	modified B-layer			B+V_O		
	I	*S*	*T*	*I*	*S*	*T*
O^{S1}	−1.61	+0.58	−1.03			
O^{S2}				−1.37	+0.21	−1.16
O^{S3}	−1.13	+0.99	−0.14	−0.55	+0.46	−0.09
O^{S4}	−1.76	+0.99	−0.77	−0.82	+0.48	−0.34

[a]The total shifts (*T*) are shown along with the decomposition into initial (*I*) and screening (*S*) parts: Δ_{SCLS}(total) = Δ(initial) + Δ(screening). The labeling of O atoms corresponds to that in Figure 10.

energy corresponding to higher/lower kinetic energy. Generally, due to the reduced coordination at the surface a positive screening contribution is expected (i.e., the core hole is less screened at the surface than in the bulk), but transition metal surfaces,[72] Si(001)[64] and RuO_2(110),[73] are cases where the opposite trend has been observed.

On the clean surface (B-layer) there are two types of oxygen ions, with (O^{S1} and O^{S4}) and without a tetrahedral neighbor (O^{S3}), which exhibit distinct behaviors. O^{S1} and O^{S4} show a negative total shift of −1.03 and −0.77 eV, respectively, whereas the SCLS of O^{S3} is only 0.14 eV. This difference is a direct result of the different coordination environments of the ions. Because O^{S3} has a coordination environment much closer to that in the bulk, it also shows a small total shift. The states near the Fermi level play a significant role in screening an ionized core. In Figure 12a we have plotted the projected density of states (PDOS) of surface oxygen ions. The O 2p band of O^{S1} shows a significant weight close to the Fermi level,

dx.doi.org/10.1021/jp3078024 | J. Phys. Chem. C 2013, 117, 2719−2733

Table 2. O 1s SCLS on Fe_3O_4(001) (in eV) for Three Different Adsorption Models: Isolated Water Molecule Dissociated in an Oxygen Vacancy Thus Forming Two Surface OH Groups ($1D_V$), a B-Layer with Two (2M) and Four H_2O Molecules (4M), Where Half of the Molecules Dissociate[a]

	$1D_V$				2M			4M		
	I	*S*	*T*		*I*	*S*	*T*	*I*	*S*	*T*
O^{S1}+H	−0.07	+1.27	+1.19	O^{S1}	−1.60	+1.04	−0.56	−1.60	+1.18	−0.42
O^{S2}+H	−0.07	+1.27	+1.20	O^{S2}	−1.39	+0.66	−0.73			
O^{S3}	−0.64	+0.34	−0.30	O^{S3}	−0.94	+0.84	−0.09			
O^{S4}	−1.27	+0.28	−0.99	O^{S4}+H	−0.43	+2.07	+1.64	−0.19	+2.12	+1.93
				$O^{(H_2O)}$	−0.27	+2.87	+2.60	−0.17	+3.10	+2.93
				$O^{(OH)}$	−1.04	+2.48	+1.44	−1.04	+2.48	+1.44

[a]The total shifts (*T*) are shown along with the decomposition into initial (*I*) and screening (*S*) parts: Δ_{SCLS}(total) = Δ(initial) + Δ(screening). The labeling of O atoms corresponds to that in Figure 10.

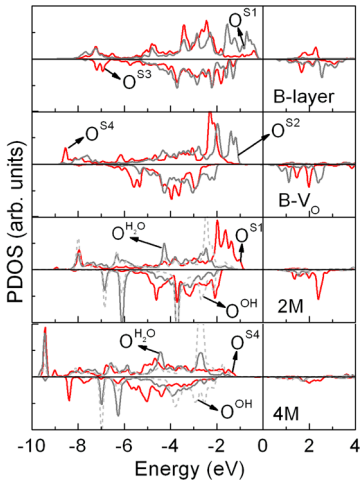

Figure 12. Projected DOS of the 2p bands of surface oxygen ions for the most stable terminations: B-layer-modified, B-layer with an oxygen vacancy (V_O), B-layer with 2 H_2O molecules in mixed adsorption, and B-layer with four H_2O molecules in mixed adsorption. For the labeling of the oxygen ions, see Figure 11.

while the PDOS of O^{S3} is much lower in this region and the center of mass is shifted to lower energies.

The ab initio surface phase diagram of magnetite(001)[30] indicates that at low oxygen partial pressures a B-layer with oxygen vacancies ($B+V_O$) is stabilized, which is consistent with the results of several experiments.[10,12,19,23,24] All surface oxygens in $B+V_O$ show negative initial and total shifts similar to the defect-free surface. The SCLS of the oxygen opposite the vacancy across the B row (O^{S4}), which exhibits a significant lateral relaxation, thereby effectively increasing its coordination, is strongly reduced to −0.34 eV. The difference in SCLS of O^{S2} and O^{S4} is again in line with the position of the O 2p peaks with respect to the Fermi level shown in Figure 12b: that of O^{S2} is closer to E_F and consequently exhibits a higher SCLS of −1.16 eV than that of O^{S4} whose O 2p peak lies lower in energy.

Both the DFT calculations[30,41] as well as the XPS results of this study and our previous ex situ XPS measurements[35] indicate dissociation of water at oxygen vacancies at low p(H_2O). Table 2 lists the SCLS for the hydroxylated oxygen vacancy ($1D_V$). We find that the total shift of O^{S1} (+1.19 eV) and O^{S2} (+1.20 eV), which are protonated, is now positive and matches closely the 1.2 eV measured in the XPS experiment at 10^{-5} Torr. Thus, the DFT calculations allow us to assign this SCLS to a hydroxyl group bound to a vacancy. Moreover, our calculations reveal that screening (+1.27 eV) is the dominant contribution to the total shift. On the other hand, the uncovered surface oxygens have a negative total shift ($\Delta_{SCLS}(O^{S3})$ = −0.33 eV, Δ_{SCLS} (O^{S4}) = −0.99 eV), much like those on the clean surface. An asymmetry of the O1s peak toward higher binding energies found in the XPS experiments (see discussion above and refs 11, 64, and 65) was attributed either to the presence of OH groups or to final state effects. From the present DFT calculations, we can confirm that the asymmetry toward lower kinetic energies is likely related to the presence of surface OH groups.

With increasing water coverage, the surface phase diagram of magnetite(001) predicts a mixed adsorption mode of water 2M and 4M, where hydrogen bonds stabilize the H_2O−OH network.[30] In the isobar experiments it was not only found that H_2O and OH uptake coincide but also that the presence of molecular H_2O cannot be ruled out on a surface covered with hydroxyls, which is consistent with a mixed adsorption mode.

The SCLSs for the partially dissociated terminations are listed in Table 2. The total shift of the surface hydroxyl (protonated surface oxygen) (O^{S4}+H) in 2M and in 4M vary between +1.64 and +1.93 eV. These values are again dominated by the screening effect, whereas the initial shifts are small. The higher total shift for protonated surface oxygen in 2M and 4M compared to $1D_V$ is attributed to the presence of different functional groups on the surface such as H_2O and OH and the formation of hydrogen bonds. On the other hand, OH groups adsorbed on top of an octahedral Fe show a total shift of +1.44 eV, which matches well with the predicted range of 1 to 1.4 eV for an OH group in the isobar experiments. The total shifts of the adsorbed H_2O molecules, which are hydrogen bonded to the OH groups, vary from +2.60 to +2.90 eV. These values are also close to the experimentally determined range of +3.0 to +3.5 eV in isobar experiments. The DFT result also matches well the measured shift of hydrogen-bonded H_2O molecules on metal and metal oxide surfaces.[47,68] The slightly higher experimental values are likely indicative of adsorption of further weakly bound water layers, which are not considered in the DFT calculations.

To further understand the influence of adsorbate−adsorbate interactions (e.g., H_2O and OH groups in 2M and 4M), we also calculated the SCLS for an isolated H_2O molecule adsorbed nearly parallel to the surface (1F, see ref 41) and for a single dissociated H_2O molecule on the surface (1D, see ref 41). The total shift of the O^{H2O} in in case of molecular adsorption (1F) is +5.06 eV, which is close to the measured shift for a gas-phase molecule in the XPS experiments. For comparison, when the water molecule contributes a hydrogen bond to a neighboring OH group in 2M, the total shift drops to +2.60 eV. For O^{H2O} in

dx.doi.org/10.1021/jp3078024 | J. Phys. Chem. C 2013, 117, 2719−2733

1F, the screening term is highest (+4.02 eV). In the dissociative adsorption of a single molecule (1D), the large initial (−1.81 eV) and screening term (+2.30 eV) result in a total shift of only +0.49 eV for O^{OH} adsorbed on top of Fe_B. This value is significantly smaller than the one (+1.44 eV) in the cases of 2M and 4M. Furthermore, the surface hydroxyl group shows a total shift of +1.40 eV. We attribute the difference in the total shift of the OH group on top of a Fe_B-ion and that of a surface hydroxyl group (formed by the protonation of a surface oxygen) to their electronegative and electropositive natures, respectively.[73] The same trend is observed in the initial shifts. Overall, our results show that the hydrogen bonded OH group on top of Fe_B has a distinct behavior compared to the surface hydroxyl. Furthermore, the interaction between neighboring H_2O molecules and OH groups in the mixed adsorption geometries influences strongly the SCLS.

Previous studies have shown the importance of screening effects.[74,75] Our SCLS calculations reveal that the final-state screening is the dominating contribution. The final-state screening is particularly high for adsorbed species such as O^{H2O} and OH groups on top of Fe_B. The projected density of states shown in Figure 12 reveals that their O 2p peak lies lower in energy than that of the hydoxylated surface oxygen atoms, indicating the poor screening of the adsorbate atoms.

The calculated work function (Φ) for the clean surface (4.85 eV) and different adsorbate configurations as a function of water coverage (expressed in number of H_2O molecules) is shown in Figure 13. In the case of mixed adsorption the work

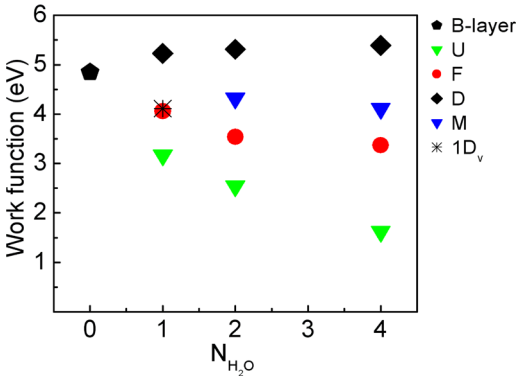

Figure 13. Work function of the clean $Fe_3O_4(001)$ surface and for different adsorbate configurations as a function of coverage. These include molecular adsorption in an upright (U) or flat (F) geometry, and mixed (M) or dissociative (D) adsorption. Additionally, the work function for a single water molecule dissociated in a surface oxygen vacancy is given ($1D_V$).

function decreases with increasing coverage and then saturates at full coverage. The trend and the reduction of the work function by ∼0.5−0.7 eV agree well with the experimental data shown in Figure 8. For comparison we have also displayed Φ for dissociated molecules, which increases with coverage, whereas molecular water adsorption in flat and particularly in upright configurations reduces significantly the work function (by up to 1.75 eV) due to the strong dipole moment of the water molecule. Similar strong reduction of Φ was found for the adsorption of hydrogen on $Fe_3O_4(001)$.[76] These adsorbate configurations (molecular and dissociative) are, however, energetically less favorable than the mixed adsorption. Thus, the change in work function can be used as an indication of a particular adsorbate mode.

For magnetite, which is a strongly correlated system, we have considered electronic correlations beyond the generalized gradient approximation[53] using an additional on-site Coulomb repulsion term[54] with U = 5 eV and J = 1 eV applied to the Fe 3d states. Similar values were previously used to describe the low temperature phase of bulk Fe_3O_4.[55,56] Using these values, GGA+U correctly describes the opening of an insulating band gap[29,30] at the $Fe_3O_4(001)$ surface, which is consistent with scanning tunneling spectroscopy measurements.[57] Previous results[41] have shown that GGA+U gives a more reliable description of the mechanism of water adsorption on the $Fe_3O_4(001)$ surface. Unlike the case of hematite(0001) ([77] and references therein), the phase diagrams of $Fe_3O_4(001)$ obtained within GGA and GGA+U give overall similar trends consistent with experiments concerning the stabilization of the modified B-layer over a broad range of pressures for the clean surface and the initial dissociation of water at oxygen defect sites, followed by a broad range of stability of a mixed adsorption mode.[30] In this paper we focus on surface core level shifts of O 1s states and to trends in the O 2p valence bands of different surface species. We note that these are less affected by the inclusion of an on-site Coulomb repulsion term on the Fe 3d states. The good overall agreement between the calculated surface core level shifts and those measured by XPS support the appropriateness of the chosen approach.

4. DISCUSSION

The experimental results of this study differ from those reported previously for an ex situ XPS study of the interaction of water vapor with the magnetite(001) surface (i.e., water dosing was performed in a separate chamber) by some of the present co-authors.[35] The chemical shift of the hydroxyl species was found to be ∼2 eV for doses at p(H_2O) higher than 10^{-4} Torr in this earlier study. This shift is about twice the value reported in the present study. In addition, hydroxyl coverages deduced from our previous data were significantly higher than in the present study. This result was taken as evidence that hydroxylation extends into the subsurface layers. We believe our previous data were affected by some undetected contaminant, which binds to the water during prolonged deposition and remains on the surface during evacuation of water from the chamber. Due to much faster data acquisition in the present study, we were in a position to routinely check for all suspect contaminants. In particular carbon-containing species, which are dominant contaminants, were monitored on a regular basis. In retrospect it is interesting to observe that the uptake curve reported in our previous study has a shape similar to the uptake curves derived for hydroxyls in the current study. We stress again that conditions in these old and new experiments are different. In our previous study, water was evacuated after each dose, whereas in the present study, the sample was continuously exposed to increasing or decreasing water pressures and remained in equilibrium with the adsorbed water layer. Although the chemical shift of the hydroxyl species from our earlier ex situ study is much higher than the value of 1.3 eV reported for (α-FeOOH), a reference model oxyhydroxide,[78] the chemical shift from the present study agrees well with this reference value. In addition, data presented in the present paper unambiguously show that under the conditions of our experiments, hydroxylation is limited to the topmost layer and does not progress to the subsurface region as suggested in our earlier paper.

dx.doi.org/10.1021/jp3078024 | J. Phys. Chem. C 2013, 117, 2719−2733

The results of this investigation demonstrate the importance of cooperative effects in water interactions on the magnetite(001) surface. Beyond the initial adsorption at vacancy sites, the dissociative adsorption of water molecules occurs only when several water molecules are present simultaneously on the surface to trigger a partial dissociation. The simultaneous presence of water and hydroxyl species on the magnetite(001) surface is particularly clearly visible in high quality (i.e., contamination free) isobars. The DFT calculations provide an explanation of this behavior: The hydrogen bonding between hydroxyl species and water molecules stabilizes the mixed adsorption mode. A similar adsorption mechanism was previously proposed for the water/MgO(100)[79] and TiO_2(110)[80] interface based on DFT calculations. The recent study of water splitting on magnetite(001) by Parkinson et al.[38] achieved very low monolayer coverages (maximum of ∼0.08 ML of surface hydroxyls) and failed to observe hydroxylation of surface iron atoms. However, the water exposures in their experiments were several orders of magnitude lower (2.25×10^2 L maximum) than those in our experiments ($(2-4) \times 10^5$ L). These low water exposures are well below the threshold $p(H_2O)$ found in our experiments ($\sim 10^{-4}$ Torr), and therefore cooperative interactions among surface water molecules do not occur. On the basis of our findings, only hydroxylation of defect sites is expected under the conditions of the Parkinson et al. study.[38]

In addition, the presence of water molecules on the magnetite(001) surface provides an explanation for the modest, but measurable, changes of the work function. As pointed out in an early review of the reaction of water with solid surfaces,[81] adsorbed hydroxyl radicals (in this paper we use the term hydroxyl also for surface hydroxide species) are not expected to decrease but rather to increase the work function. This expectation is in agreement with our DFT calculations for magnetite(001), which show a slight increase of the work function for hydroxyl species. On the other hand, even a simple model based on a dipolar picture of water molecules predicts large reductions, on the order of a few eV, of the work function for the molecular adsorption of water, in particular for the upright adsorption mode. Indeed the DFT results show a reduction of up to 1.75 eV for upright adsorption depending on concentration of the molecules. On the other hand, the reduction of $\Delta\Phi$ is smaller when the water molecule is tilted from the surface normal related to change in orientation of the dipole moment of the molecule with respect to the surface and depolarization due to hydrogen bonding. The good agreement of our experimental data (which show an initial decrease of the work function by 0.4 eV) with theory (which derives a change of 0.5−0.7 eV) provides strong support for a mixed adsorption model on the (001) surface of magnetite. In part due to the large width of the O 1s XPS peak, it is very difficult to derive SCLS for metal oxide surfaces from experimental data. In fact, we are aware of only one previous study which reports surface shifts for a metal oxide, a fractured cuprite (Cu_2O),[82] for which two additional components were found to be shifted by ∼1 eV to higher and lower binding energy relative to the bulk component and were assigned to hydroxyl and undercoordinated surface oxygen species, respectively. For the clean Fe_3O_4(001) surface, the DFT calculations presented here show SCLS ranging from −0.14 to −1.03 eV depending on the coordination of surface oxygen. Because of the large widths, we are unable to derive directly the surface shift for oxygen species. However, the presence of such a shift can be inferred indirectly from the narrowing of the O 1s line after adsorption of a probe molecule (in our case water molecules), which, by binding hydrogen atoms, partially relieves the undercoordination of the surface oxygen atoms. In addition, as our present calculations clearly show for complex surface superstructures, there is no single core-level shift. Instead, the shifts depend sensitively on the local coordination of O surface atoms, and in particular shifts for atoms bound to or distant from tetrahedral Fe atoms in the second layer are quite dissimilar (see Figure 10 and Table 3). An additional layer of complexity is related to the presence of O vacancies and their high propensity to hydroxylate. Our surface preparation is likely to introduce some vacancies and therefore facilitate the formation of surface hydroxyl species upon exposure of magnetite(001) to water vapor. This is evidenced in Figure 7 at low RH, where the surface contains approximately 20% of a monolayer of hydroxyls associated with water dissociation at defect sites. The DFT calculation for magnetite(001) shows that under reducing conditions, oxygen vacancies are likely to be formed on a clean surface and, in addition, that the latter are favorable sites for water dissociation. Our experimental chamber was dedicated to consecutive water experiments; therefore, despite a good base pressure (10^{-10} Torr at the beginning of the experiment but reduced to 10^{-9} Torr after prolonged water dosing experiments), the presence of hydroxyls cannot be avoided. In addition, because the enthalpy of hydroxyl formation is very high, hydroxyls are difficult to remove thermally.

Table 3. O 1s SCLS of the Surface Oxygen O^{S4} 9 (eV) from Seven Different Models[a]

Δ_{SCLS} (O^{S4})	initial	screening	total
mod. B-layer	−1.76	+0.99	−0.77
B+V_O	−0.82	+0.48	−0.34
1F	−1.73	+0.97	−0.76
1D (H)	−0.49	+1.89	+1.40
$1D_V$	−1.27	+0.28	−0.99
2M (H)	−0.43	+2.07	+1.64
4M (H)	−0.19	+2.12	+1.93

[a]The surface oxygen S4 is labeled in Figure 10. The variation of SCLS with the changing surroundings in each adsorption model is clearly seen. The total shifts are shown along with its decomposition into initial and screening part. Δ_{SCLS}(total) = Δ(initial) + Δ(screening). Protonation of O^{S4} is denoted by (H).

The main goal of this work was to study the reaction of water vapor with the magnetite(001) surface. As mentioned above, a clean but defective surface is prone to hydroxylation just after first exposure to water vapor. This effect was observed in our recent ambient pressure XPS investigation of the interaction of water with the (0001) surface of hematite.[47] Only the clean surface of hematite at the beginning of a series of spectral measurements prior to water dosing yields a symmetric O 1s spectrum. Hydroxylation of defect sites occurs immediately after the first water dose at pressures as low as 10^{-8} Torr of water, and the spectra remain unchanged until the onset of terrace site hydroxylation at much higher water vapor pressures. Similarly, in the present study, the (001) surface of magnetite yields almost identical O 1s spectra, which are consistent with partial hydroxylation of the surface, preferentially at defect sites, until hydroxylation of terrace sites becomes the dominant mode of adsorption for higher RHs (water vapor pressures). The

dx.doi.org/10.1021/jp3078024 | J. Phys. Chem. C 2013, 117, 2719−2733

experimentally measured binding energy shift of the O 1s peak assigned to hydroxyl species bound at vacancies is in excellent agreement with the results of our DFT calculations. Also, values of the shift for hydroxyls and molecular water for the mixed adsorption mode agree well with theory. The DFT calculations show that the total core-level shifts result from large final-state effects. The experimental analysis applies an approximation of the least amount of distinguishable contributions in the spectra. In our analysis, we considered only three peaks − from the substrate lattice oxygens, OH, and H_2O. These peaks may well be envelopes of several components resulting from atoms in dissimilar local bonding configurations, which cannot be resolved unambiguously based on the available data. In view of these limitations, we likely cannot distinguish OH groups bonded to iron and OH groups formed by protonating surface O atoms. For these, our DFT calculations show a chemical shift of surface and adsorbed hydroxyl groups varying between +1.2 and +1.9 eV. We note that the SCLS of water for the mixed adsorption (2.6−2.9 eV) are somewhat lower than the experimental values (3.0−3.5 eV). We attribute this difference to the fact that in the simulations we have considered coverages only up to four H_2O molecules per surface unit cell, where all FeB-sites are saturated. In contrast, the coverage in the experiments is much higher, where between one and two molecular water layers adsorb on top of the initially hydroxylated surface. As discussed in section 3b, the calculated SCLS of a weakly bound water molecule is 5.06 eV. Furthermore, it is likely that enhanced water coverage not considered in the DFT study triggers further dissociation processes, eventually leading to a fully hydroxylated layer covered by water molecules.

In many respects the results of the present study agree with those from earlier studies of water adsorption on the (111) magnetite surface.[83−87] In both cases water readily dissociates on the surface, and OH/H_2O species coexist at intermediate RHs bound to the surface as well as to each other through hydrogen bonding. Finally, in both cases the surfaces are terminated by increasing amounts of water at high RHs. These changes of RH are achieved in the present study by increasing the water vapor pressures for isotherms or reducing temperature to the ambient range for isobars. In the studies by Joseph et al.,[83,84] which were conducted at very low water vapor pressures (10^{-8}−10^{-6} mbar), these changes occur by major decreases of the temperature to the cryogenic regime. The detailed assessment of the role of the pressure gap in observed behavior is difficult due to the different crystallographic orientation and surface terminations. It is likely that the surface orientation rather than the pressure gap is responsible for some detailed differences in the results. For example, our DFT calculations[30,41] show that hydroxylation of single water molecules occurs at vacancies. In contrast, the DFT study of Grillo et al.[87] predicted that a single water molecule dissociates easily on the Fe terrace site.

5. CONCLUSIONS

We have studied the reaction of water vapor with the $(2^{1/2}\times2^{1/2})R45°$ reconstructed surface of $Fe_3O_4(001)$ with ambient-pressure XPS and DFT. The core-level O 1s spectra provide information on equilibrium substrate−water interactions over a broad range of $p(H_2O)$ and RH. On the basis of isotherms measured at near ambient temperatures, water was found to dissociatively adsorb at pressures above 10^{-4} Torr. At ~10^{-2} Torr hydroxyl coverage, saturation is close to 1 ML. The isobars also show a reproducible, well-defined hydroxylation threshold at a RH of 10^{-2}%. The hydroxylation also marks an increase of water coverage, which continues after hydroxyl coverage saturates at ~1 ML at RH = 0.1%. Our results demonstrate a cooperative effect in the interaction of water with the magnetite(001) surface, i.e., promotion of hydroxylation coincides with condensation of water. The chemical shifts of the hydroxyl species derived from the O 1s spectra vary between 1 and 1.4 eV, with an average value of ~1.2 eV. This result agrees well with chemical shifts in iron oxyhydroxides such as goethite (~1.3 eV),[78] but it differs from all prior UHV photoemission studies of hydroxylated magnetite [mostly on the (111) surface[35,65,84]]. The chemical shift for water varies from 3.0 to 3.5 eV and coverage exceeds ~1 ML at RH ~ 40%. A 30% narrowing of O 1s peak of the substrate (fwhm) with an increase of relative humidity suggests quenching of the chemical shift of the clean surface relative to the bulk. The similarity of isobar (with little C surface contamination) and isotherm (with C surface contamination) XPS data and DFT results on C-free magnetite(001) indicate that surface hydroxylation is not catalyzed by the presence of spectator carbonaceous species.

In addition, the DFT calculations of the clean and water-reacted $Fe_3O_4(001)$ surfaces predict O 1s surface core-level shifts of 1.4 and 3 eV for hydroxyl and surface water, respectively, which is in good agreement with our experimental results. Additionally, the work function of the clean and water-covered magnetite(001) surfaces were determined. The decrease of the work function for mixed water adsorption by 0.5 eV agrees well with values measured experimentally.

AUTHOR INFORMATION

Corresponding Author

*E-mail: gordon.brown@stanford.edu.

Present Address

#Department of Chemistry & Biochemistry, University of Delaware, Newark, DE 19716.

Notes

The authors declare no competing financial interest.

ACKNOWLEDGMENTS

This work was supported by the U.S. National Science Foundation through Grant CHE-0431425 (Stanford Environmental Molecular Science Institute) and BaCaTeC (Bavaria California Technology Center). Work was performed on beamline 11.0.2 at the Advanced Light Source of Lawrence Berkeley National Laboratory, which is supported by the Director, Office of Science, Office of Basic Energy Sciences, Division of Chemical Sciences, Geosciences, and Energy Biosciences of the U.S. Department of Energy under contract no. DE-AC02-05CH11231. The DFT calculations were performed at the Leibniz Rechenzentrum, Garching (project h0721).

REFERENCES

(1) Cornell, R. M.; Schwertmann, U. *The Iron Oxides; Structure Properties, Reaction, Occurrences and Uses*; Wiley-VCH: New York, 2003.

(2) Wiatrowski, H. A.; Das, S.; Kukkadapu, R.; Ilton, E. S.; Barkay, T.; Yee, N. Reduction of Hg(II) to Hg(0) by magnetite. *Environ. Sci. Technol.* **2009**, *43*, 5307−5313.

(3) Bibes, M.; Barthélémy, A. Oxide spintronics. *IEEE Trans. Electron Devices* **2007**, *54*, 1003−1023.

(4) Walz, F. The Verwey transition – a topical review. *J. Phys.: Condens. Matter* **2002**, *14*, R285–R340.
(5) Fleet, M. E. The structure of magnetite . *Acta Crystallogr., Sect. C: Cryst. Struct. Commun.* **1981**, *40*, 917–920.
(6) Tarrach, G.; Burgler, D.; Schaub, T.; Wiesendanger, R.; Guntherodt, H.-J. Atomic surface-structure of Fe_3O_4(001) in different preparation stages studied by scanning tunneling microscopy. *Surf. Sci.* **1993**, *285*, 1–14.
(7) Coey, J. M. D.; Shvets, I. V.; Wiesendanger, F. L; Guntherodt, H.-J. Charge freezing and surface anisotropy on magnetite(100). *J. Appl. Phys.* **1993**, *73*, 6742–6744.
(8) Gaines, J. M.; Bloemen, P. J. H.; Kohlhepp, J. T.; Bulle-Lieuwma, C. W. T.; Wolf, R. M.; Reinders, A.; Jungblut, R. M.; van der Heijden, P. A. A.; van Eemeren, J. T. W. M.; de Stegge, J.; et al. An STM study of Fe_3O_4(100) grown by molecular beam epitaxy. *Surf. Sci.* **1997**, *373*, 85–94.
(9) Seoighe, C.; Naumann, J.; Shvets, I. V. Studies of surface structures on single crystalline magnetite (100). *Surf. Sci.* **1999**, *440*, 116–124.
(10) Voogt, F. C.; Fujii, T.; Smulders, P. J. M.; Niesen, L.; James, M. A.; Hibma, T. NO_2-assisted molecular-beam epitaxy of Fe_3O_4, delta-Fe_3O_4, and gamma-Fe_2O_3 thin films on MgO(100). *Phys. Rev. B* **1999**, *60*, 11193–11206.
(11) Chambers, S. A.; Thevuthasan, S.; Joyce, S. A. Surface structure of MBE-grown Fe_3O_4(001) by X-ray photoelectron diffraction and scanning tunneling microscopy. *Surf. Sci.* **2000**, *450*, L273–L279.
(12) Stanka, B.; Hebenstreit, W.; Diebold, U.; Chambers, S. A. Surface reconstruction of Fe_3O_4(001). *Surf. Sci.* **2000**, *448*, 49–63.
(13) Mariotto, G.; Murphy, S.; Shvets, I. V. Charge ordering on the surface of Fe_3O_4(001) *Phys. Rev. B* [online] **2002**, *66*, article 245426.
(14) Mariotto, G.; Ceballos, S. F.; Murphy, S.; Shvets, I. V. Scanning tunneling microscopy studies of the Fe_3O_4(001) surface using antiferromagnetic probes. *J. App. Phys.* **2003**, *93*, 7142–7144.
(15) Ceballos, S. F.; Mariotto, G.; Jordan, K.; Murphy, S.; Seoighe, C.; Shvets, I. V. An atomic scale STM study of the Fe_3O_4(001) surface. *Surf. Sci.* **2004**, *548*, 106–116.
(16) Shvets, I. V.; Mariotto, G.; Jordan, K.; Berdunov, N.; Kantor, R.; Murphy, S. Long-range charge order on the Fe_3O_4(001) surface. *Phys Rev. B* [online] **2004**, *70*, article 155406.
(17) Jordan, K.; Mariotto, G.; Ceballos, S. F.; Murphy, S.; Shvets, I. V. Spin polarized STM imaging of the Fe_3O_4(001) surface using antiferromagnetic tips. *J. Magn. Magn. Mater.* **2005**, *290–291*, 1029–1032.
(18) Jordan, K.; Murphy, S.; Shvets, I. V. Initial nucleation of Au on the R45° reconstructed Fe_3O_4(001) surface. *Surf. Sci.* **2006**, *600*, 5150–5157.
(19) Subagyo, A.; Sueoka, K. Defect-induced charge freezing on epitaxial Fe_3O_4(001) film surfaces studied by spin-polarized scanning tunneling microscopy. *Jpn. J. Appl. Phys.* **2005**, *44*, 5447–5450. Subagyo, A.; Sueoka, K.; Mukasa, K. Reconstruction and charge ordering of epitaxial Fe_3O_4(001) films. *J. Magn. Magn. Mater.* **2005**, *290–291*, 1037–1039.
(20) Fonin, M.; Pentcheva, R.; Dedkov, Y. S.; Sperlich, M.; Vyalikh, D. V.; Scheffler, M.; Rüdiger, U.; Güntherodt, G.Surface electronic structure of the Fe_3O_4(100): Evidence of a half-metal to metal transition. *Phys Rev. B* [online] **2005**, *72*, article 104436.
(21) Murphy, S.; Ceballos, S. F.; Mariotto, G.; Berdunov, N.; Jordan, K.; Shvets, I. V.; Mukovskii, Y. M. Atomic scale spin-dependent STM on magnetite using antiferromagnetic STM tips. *Microsc. Res. Technol.* **2005**, *66*, 85–92.
(22) Stoltz, D.; Onsten, A.; Karlsson, U. O.; Gothelid, M. Scanning tunneling microscopy of Fe- and O-sublattices on Fe_3O_4(100). *Ultramicroscopy* **2008**, *108*, 540–544.
(23) Subagyo, A.; Sueoka, K. Spin-polarized scanning tunneling microscopy study on charge ordering of reconstructed Fe_3O_4(001) film surfaces . *Jpn. J. Appl. Phys., Part 1* **2006**, *45*, 2255–2258.
(24) Subagyo, A.; Sasaki, Y.; Oka, H.; Sueoka, K. Inhomogeneous surface electronic properties and charge ordering in epitaxial Fe_3O_4 films on MgO(001). *Phys. Status Solidi B* **2007**, *244*, 4482–4485.
(25) Spiridis, N.; Handke, B.; Slezak, T.; Barbasz, J.; Zajac, M.; Haber, J.; Korecki, J. Surface structure of epitaxial magnetite Fe_3O_4(001) films: In situ STM and CEMS studies. *J. Phys. Chem. B* **2004**, *108*, 14356–14361.
(26) Spiridis, N.; Barbasz, J.; Łodziana, Z.; Korecki, J. Fe_3O_4(001) films on Fe(001): Termination and reconstruction of iron-rich surfaces. *Phys Rev. B* [online] **2006**, *74*, article 155423.
(27) Pentcheva, R.; Wendler, F.; Meyerheim, H. L.; Moritz, W.; Jedrecy, N.; Scheffler, M. Jahn-Teller stabilization of a polar metal oxide surface: Fe_3O_4(001). *Phys. Rev. Lett.* [online] **2005**, *94*, article 126101.
(28) Cheng, C. Structure and magnetic properties of the Fe_3O_4(001) surface: Ab initio studies. *Phys Rev. B* [online] **2005**, *71*, article 052401.
(29) Łodziana, Z. Surface Verwey transition in magnetite. *Phys. Rev. Lett.* [online] **2007**, *99*, article 206402.
(30) Mulakaluri, N.; Pentcheva, R.; Wieland, M.; Moritz, W.; Scheffler, M. Partial dissociation of water on Fe_3O_4(001): Adsorbate induced charge and orbital order. *Phys. Rev. Lett.* [online] **2009**, *103*, article 176102.
(31) Tasker, P. W. Stability of ionic-crystal surfaces. *J. Phys. C: Solid State Phys.* **1979**, *12*, 4977–4984.
(32) Goniakowski, J.; Finocchi, F.; Noguera, C. Polarity of oxide surfaces and nanostructures. *Rep. Prog. Phys.* [online] **2008**, *71*, article 016501.
(33) LaFemina, J. P. Oxide Surfaces. *CRC Crit. Rev. Surf. Chem.* **1994**, *3*, 297–383.
(34) Pentcheva, R.; Pickett, W. E. Electronic phenomena at complex oxide interfaces: insights from first principles. *J. Phys.: Condens. Matter* [online] **2010**, *22*, article 043001, and see references therein.
(35) Kendelewicz, T.; Liu, P.; Doyle, C. S.; Brown, G. E., Jr.; Nelson, E. J.; Chambers, S. A. Reaction of water with the (100) and (111) surfaces of Fe_3O_4. *Surf. Sci.* **2000**, *453*, 32–46.
(36) Liu, P.; Kendelewicz, T.; Brown, G. E., Jr.; Nelson, E. J.; Chambers, S. A. Reaction of water with α-Al_2O_3 and α-Fe_2O_3 (0001) surfaces: synchrotron x-ray photoemission studies and thermodynamic calculations. *Surf. Sci.* **1998**, *417*, 53–65.
(37) Peden, C. H. F.; Herman, G. S.; Ismagilov, I. Z.; Kay, B. D.; Henderson, M. A.; Kim, Y.-J.; Chambers, S. A. Model catalyst studies with single crystals and epitaxial thin oxide films. *Catal. Today* **1999**, *51*, 513–519.
(38) Parkinson, G. S.; Novotny, Z.; Jacobson, P.; Schmid, M.; Diebold, U. Room temperature water splitting at the surface of magnetite. *J. Am. Chem. Soc.* **2011**, *133*, 12650–12655.
(39) Rustad, J. R.; Felmy, A. R.; Bylaska, E. J. Molecular simulation of the magnetite-water interface. *Geochim. Cosmochim. Acta* **2003**, *67*, 10001–10016.
(40) Kundu, T. K.; Rao, K. H.; Parker, S. C. Atomistic simulation studies of magnetite surface structures and adsorption behavior in the presence of molecular and dissociated water and formic acid. *J. Colloid Interface Sci.* **2006**, *295*, 364–373.
(41) Mulakaluri, N.; Pentcheva, R.; Scheffler, M. Coverage-dependent adsorption mode of water on Fe_3O_4(001): Insights from first principles calculations. *J. Phys. Chem. C* **2010**, *114*, 11148–11156.
(42) Wang, X. G.; Weiss, W.; Shaikhutdinov, S. K.; Ritter, M.; Petersen, M.; Wagner, F.; Schlogl, R.; Scheffler, M. The hematite (alpha-Fe_2O_3) (0001) surface: Evidence for domains of distinct chemistry. *Phys. Rev. Lett.* **1998**, *81*, 1038–1041.
(43) Reuter, K.; Scheffler, M. Composition, structure, and stability of RuO_2(110) as a function of oxygen pressure. *Phys. Rev. B* [online] **2002**, *65*, article 035406.
(44) Bluhm, H.; Andersson, K.; Araki, T.; Benzerara, K.; Brown, G. E., Jr.; Dynes, J. J.; Ghosal, S.; Gilles, M. K.; Hansen, H. C.; Hemminger, J. C.; et al. Soft x-ray microscopy and spectroscopy using the Molecular Environmental Science Beamline at the Advanced Light Source. *J. Electron Spectrosc. Relat. Phenom.* **2006**, *150*, 86–104.
(45) Ogletree, D. F.; Bluhm, H.; Hebenstreit, E. L. D.; Salmeron, M. Photoelectron spectroscopy under ambient pressure and temperature

conditions. *Nucl. Instrum. Methods Phys. Res., Sect. A* **2009**, *601*, 151−160.
(46) Newberg, J. T.; Starr, D. E.; Yamamoto, S.; Kaya, S.; Kendelewicz, T.; Mysak, E. R.; Posgaard, S.; Salmeron, M. B.; Brown, G. E., Jr.; Nilsson, A.; et al. Formation of hydroxyl and water layers on MgO films studied with ambient pressure XPS. *Surf. Sci.* **2011**, *605*, 89−94.
(47) Yamamoto, S.; Kendelewicz, T.; Bluhm, H.; Ketteler, G.; Starr, D. E.; Andersson, K.; Ogasawara, H.; Salmeron, M.; Brown, G. E., Jr.; Nilsson, A. Water adsorption on α-Fe_2O_3(0001) at near ambient conditions. *J. Phys. Chem. C* **2010**, *114*, 2256−2266.
(48) Fadley, C. S.; Baird, J.; Siekhaus, W.; Novakov, T.; Bergstrom, L. Surface analysis and angular distributions in x-ray photoelectron spectroscopy. *J. Electron Spectrosc. Relat. Phenom.* **1974**, *4*, 93−137.
(49) McCafferty, E.; Wightman, J. P. Determination of the concentration of surface hydroxyl groups on metal oxide films by a quantitative XPS method. *Surf. Interface Anal.* **1998**, *26*, 549−564.
(50) While the coverage determined by this method has to be treated as an approximation, as seen from Figure 6 an OH thickness of 3.02 Å gives rise to a saturated hydroxyl surface. Thus, while the interface is likely structurally different than that of goethite, the overall surface coverage by hydroxyls is comparable. See Ewing, G. E. Ambient thin film water on insulator surfaces. *Chem. Rev.* **2006**, *106*, 1511−1526.
(51) Yang, H.; Lu, R.; Downs, R. T.; Costin, G. Goethite, alpha-FeO(OH), from single-crystal data. *Acta Crystallogr., Sect. E: Struct. Rep. Online* **2006**, *62*, 1250−1252.
(52) Blaha, P.; Schwarz, K.; Madsen, G. K. H.; Kvasnicka, D.; Luitz, J. WIEN2k: An Augmented Plane Wave + Local Orbitals Program for Calculating Crystal Properties; Karlheinz Schwarz, Technische Universität Wien, Wien, Austria, 2001; ISBN 3-9501031-1-2.
(53) Perdew, J. P.; Burke, K.; Ernzerhof, M. Generalized gradient approximation made simple. *Phys. Rev. Lett.* **1996**, *77*, 3865−3868.
(54) Anisimov, V. L.; Solovyev, I. V.; Korotin, M. A.; Czyzyk, M. T.; Sawatzky, G. A. Density functional theory and NiO photoemission spectra. *Phys. Rev. B* **1993**, *48*, 16929−16933.
(55) Leonov, I.; Yaresko, A. N.; Antonov, V. N.; Korotin, M. A.; Anisimov, V. I. Charge and orbital order in Fe_3O_4. *Phys. Rev. Lett.* [online] **2004**, *93*, article 146404.
(56) Jeng, H.-T.; Guo, G. Y.; Huang, D. J. Charge-orbital ordering and verwey transition in magnetite. *Phys. Rev. Lett.* [online] **2004**, *93*, article 156403.
(57) Jordan, K.; Cazacu, A.; Manai, G.; Ceballos, S. F.; Murphy, S.; Shvets, I. V. Scanning tunneling spectroscopy study of the electronic structure of Fe_3O_4 surfaces. *Phys. Rev. B* [online] **2006**, *74*, article 085416.
(58) Spanjaard, D.; Guillot, C.; Desjonqueres, M. C.; Treglia, G.; Lecante, J. Surface core level spectroscopy of transition metals: A new tool for the determination of their surface structure. *Surf. Sci. Rep.* **1985**, *5*, 1−85.
(59) Slater, J. C. *Quantum Theory of Molecules and Solids*; McGraw-Hill: New York, 1974; Vol. *4*, International Series in Pure and Applied Physics.
(60) Janak, J. F. Proof that delta-e-delta-Ni = episolon-i in density-functional theory. *Phys. Rev. B* **1978**, *18*, 7165−7168.
(61) Lizzit, S.; Baraldi, A.; Groso, A.; Reuter, K.; Ganduglia-Pirovano, M. V.; Stampfl, C.; Scheffler, M.; Stichler, M.; Keller, C.; Wurth, W. Surface core-level shifts of clean and oxygen-covered Ru(0001). *Phys. Rev. B* **2001**, *63*, article 205419.
(62) Göransson, C.; Olovsson, W.; Abrikosov, I. A. Numerical investigation of the validity of the Slater-Janak transition-state model in metallic systems. *Phys Rev. B* [online] **2005**, *72*, article 134203.
(63) Methfessel, D.; Hennig, D.; Scheffler, M. Enhanced screening of core holes at transition-metal surfaces. *Surf. Rev. Lett.* **1995**, *2*, 197−201.
(64) Wandelt, K. Photoemission studies of adsorbed oxygen and oxide layers. *Surf. Sci. Rep.* **1982**, *2*, 1−121.
(65) Cutting, R. S.; Muryn, C. A.; Vaughan, D. J.; Thornton, G. Substrate-termination and H_2O-coverage dependent dissociation of H_2O on Fe_3O_4(111). *Surf. Sci.* **2008**, *602*, 1155−1165.
(66) Fujii, T.; de Groot, F. M. F.; Sawatzky, G. A.; Voogt, F. C.; Hibma, T.; Okada, K. In situ analysis of various iron oxide films grown by NO_2-assisted molecular-beam epitaxy. *Phys. Rev. B* **1999**, *59*, 3195−3202.
(67) Relative humidity (RH%) is defined as $p/p_v(T) \times 100$, where p_v is the equilibrium vapor pressure of bulk water or ice at the corresponding temperature.
(68) Yamamoto, S.; Bluhm, H.; Andersson, K.; Ketteler, G.; Ogasawara, H.; Salmeron, M.; Nilsson, A. In situ x-ray photoelectron spectroscopy studies of water on metals and oxides at ambient conditions. *J. Phys.: Condens. Matter* [online] **2008**, *20*, article 184025.
(69) Bluhm, H. Photoelectron spectroscopy of surfaces under humid conditions. *J. Electron Spectrosc. Relat. Phenom.* **2010**, *177*, 71−84.
(70) Pentcheva, R.; Moritz, W.; Rundgren, J.; Frank, S.; Schrupp, D.; Scheffler, M. A combined DFT/LEED-approach for complex oxide surface structure determination: Fe_3O_4(001). *Surf. Sci.* **2008**, *602*, 1299−1305.
(71) Petitto, S. C.; Tanwar, K. S.; Ghose, S. K.; Eng, P. J.; Trainor, T. P. Surface structure of magnetite (111) under hydrated conditions by crystal truncation rod diffraction. *Surf. Sci.* **2010**, *604*, 1082−1093.
(72) Reuter, K.; Scheffler, M. Surface core-level shifts at an oxygen-rich Ru surface: O/Ru(0001) vs. RuO_2(110). *Surf. Sci.* **2001**, *490*, 20−28.
(73) Tamura, H.; Katayama, N.; Furuichi, R. Modeling of ion-exchange reactions on metal oxides with the Frumkin isotherm.1. Acid-base and charge characteristics of MnO_2, TiO_2, Fe_3O_4, and Al_2O_3 surfaces and adsorption affinity of alkali metal ions. *Environ. Sci. Technol.* **1996**, *30*, 1198−1204.
(74) Pehlke, E.; Scheffler, M. Evidence for site-sensitive screening of core holes at the Si and Ge (001) surface. *Phys. Rev. Lett.* **1993**, *71*, 2338−2341.
(75) Andersen, J. N.; Henning, D.; Lundgren, E.; Methfessel, M.; Nyholm, R.; Scheffler, M. Surface core-level shifts of some 4d-metal single-crystal surfaces: Experiments and ab initio calculations. *Phys. Rev. B* **1994**, *50*, 17525−17533.
(76) Mulakaluri, N.; Pentcheva, R. Hydrogen adsorption and site-selective reduction of the Fe_3O_4(001) surface: Insights from first principles. *J. Phys. Chem. C* **2012**, *116*, 16447−16453.
(77) Barbier, A.; Stierle, A.; Kasper, N.; Guittet, M.-J.; Jupille, J. Surface termination of hematite at environmental oxygen pressures: Experimental surface phase diagram. *Phys Rev. B* [online] **2007**, *75*, article 233406.
(78) Rakovan, J.; Becker, U.; Hochella, M. F., Jr. Aspects of goethite surface microtopography, structure, chemistry, and reactivity. *Am. Mineral.* **1999**, *84*, 884−894.
(79) Giordano, L.; Goniakowski, J.; Suzanne, J. Partial dissociation of water molecules in the (3 × 2) water monolayer deposited on the MgO (100) surface. *Phys. Rev. Lett.* **1998**, *81*, 1271−1273.
(80) Lindan, P. J. D.; Harrison, N. M.; Gillan, M. J. Mixed dissociative and molecular adsorption of water on the rutile (110) surface. *Phys. Rev. Lett.* **1998**, *80*, 762−765.
(81) Thiel, P. A.; Madey, T. E. The interaction of water with solid surfaces − fundamental aspects. *Surf. Sci. Rep.* **1987**, *7*, 211−385.
(82) Harmer, L.; Skinner, W. M.; Buckley, A. N.; Fan, L.-J. Species formed at cuprite fracture surfaces: observation of O 1s surface core level shift. *Surf. Sci.* **2009**, *603*, 537−545.
(83) Joseph, Y.; Kuhrs, C.; Ranke, W.; Ritter, M.; Weiss, W. Adsorption of water on FeO(111) and Fe_3O_4(111): identification of active sites for dissociation. *Chem. Phys. Lett.* **1999**, *314*, 195−202.
(84) Joseph, Y.; Kuhrs, C.; Ritter, M.; Weiss, W. Adsorption of water on Fe_3O_4(111) studied by photoelectron and thermal desorption spectroscopy. *Surf. Sci.* **1999**, *433*−*435*, 114−118.
(85) Joseph, Y.; Kuhrs, C.; Ritter, M.; Weiss, W. Water on FeO(111) and Fe_3O_4(111): Adsorption behavior on different surface terminations. *J. Phys. Chem. B* **2000**, *104*, 3224−3236.
(86) Ranke, W.; Joseph, Y. Determination of adsorption energies and kinetic parameters by isosteric methods. *Phys. Chem. Chem. Phys.* **2002**, *4*, 2483−2498.

(87) Grillo, M. E.; Finnis, M. W.; Ranke, W. Surface structure and water adsorption on $Fe_3O_4(111)$: Spin-density functional theory and on-site Coulomb interactions. *Phys. Rev. B* [online] **2008**, *77*, article 075407.